Bone Reports 12 (2020) 100253

Contents lists available at ScienceDirect

Bone Reports

journal homepage: www.elsevier.com/locate/bonr

No evidence for alteration in early secondary mineralization by either alendronate, teriparatide or combination of both in transiliac bone biopsy samples from postmenopausal osteoporotic patients

Barbara M. Misof[a,*], Paul Roschger[a], Hua Zhou[b], Jeri W. Nieves[c,d], Mathias Bostrom[b,d], Felicia Cosman[e], Robert Lindsay[b,e], Klaus Klaushofer[a], David W. Dempster[b,f]

[a] Ludwig Boltzmann Institute of Osteology at Hanusch Hospital of OEGK and AUVA Trauma Centre Meidling, 1st Med. Dept. Hanusch Hospital, Vienna, Austria
[b] Regional Bone Center and Clinical Research Center, Helen Hayes Hospital, West Haverstraw, NY, USA
[c] Department of Epidemiology, Columbia University, New York, NY, USA
[d] Hospital for Special Surgery, New York, NY, USA
[e] Department of Medicine, Columbia University, New York, NY, USA
[f] Department of Pathology and Cell Biology, Columbia University, New York, NY, USA

ARTICLE INFO

Keywords:
Bone matrix mineralization
Combined therapy with alendronate and teriparatide
Quadruple labelling
Secondary mineralization
Transiliac bone biopsy

ABSTRACT

The influence of treatment with alendronate (ALN), teriparatide (TPTD) or concurrent treatment with both on the human bone matrix mineralization has not yet been fully elucidated. For this purpose we analyzed quadruple fluorochrome labelled transiliac bone biopsy samples ($n = 66$) from postmenopausal osteoporotic women with prior and ongoing ALN (ALN-Rx arm) or without ALN (Rx-Naïve arm) after 7 months treatment with cyclic or daily TPTD or without TPTD using quantitative backscattered electron imaging and confocal scanning laser microscopy. Additionally to the bone mineralization density distribution (BMDD) of entire cancellous and cortical compartments, we measured the mineralization kinetics, i.e. the calcium concentration between the younger (Ca_DL2) and older double labels (Ca_DL1), and in interstitial bone (Ca_int) in a subset of the biopsy cohort.

We found the BMDD from the patients with prior and ongoing ALN generally shifted to higher calcium concentrations compared to those without ALN (average degree of mineralization in cancellous bone Cn.CaMean + 3.1%, $p < 0.001$). The typical BMDD changes expected by cyclic or daily TPTD treatment due to the increased bone turnover/formation, e.g. an increase in low mineralized bone area were not observed. Additionally, we found no influence of treatment with ALN or TPTD or combination thereof on Ca_DL2, Ca_DL1, or Ca_int. Pooling the information from all groups, Ca_DL1 was +5.9% ($p < 0.001$) higher compared to Ca_DL2, corresponding to a mineralization rate of 0.18 wt% Ca per week during the early secondary mineralization process.

Our data suggest that the patients in the ALN-Rx arm had more highly mineralized bone matrix than those without ALN due to their lower bone turnover. The reason for the unexpected BMDD findings in the TPTD treated remain unknown and cannot be attributed to altered mineralization kinetics as no differences in the time course of early secondary mineralization were observed between the treatment groups.

1. Introduction

Antiresorptive and anabolic treatment have different effects on bone matrix mineralization (Dempster et al., 2016a; Roschger et al., 2014). In particular, antiresorptive treatment with bisphosphonates reduces bone turnover/formation and increases the time for secondary mineralization in bone packets and reduces the amount of newly formed bone packets. These effects together cause, on average, higher and more homogeneously mineralized bone matrix. On the other hand, anabolic treatment with teriparatide (TPTD) or PTH(1–84) lead to an increase in newly formed bone packets and an increase in bone turnover which, on average reduces bone tissue age and bone matrix mineralization density. Apart from these effects on bone matrix mineralization which are the consequence of bone formation/turnover changes due to treatment, the bone matrix mineralization might also be affected by changes in the mineralization kinetics. The latter is the time course of mineral

* Corresponding author at: Ludwig Boltzmann Institute of Osteology, UKH Meidling, Kundratstr. 37, A-1120 Vienna, Austria.
E-mail address: barbara.misof@osteologie.lbg.ac.at (B.M. Misof).

https://doi.org/10.1016/j.bonr.2020.100253
Received 11 January 2020; Accepted 26 February 2020
Available online 27 February 2020
2352-1872/ © 2020 The Authors. Published by Elsevier Inc. This is an open access article under the CC BY-NC-ND license (http://creativecommons.org/licenses/BY-NC-ND/4.0/).

accumulation within newly formed bone matrix up to the final plateau level of mineralization (primary and secondary mineralization processes). While some information on the mineralization kinetics is available from animal models (Fuchs et al., 2011; Fuchs et al., 2008; Bala et al., 2010), information from human bone samples, in particular due to treatment, is sparse so far.

Additionally to the little knowledge considering the mineralization kinetics generally, information on overall bone matrix mineralization after combined therapy is lacking. Clinical outcomes (including the gain in bone mineral density or the suppression of the well-known increase in cortical bone porosity after PTH or TPTD) indicate that combination therapy might have a benefit over mono-therapy with either the anabolic or the antiresorptive agent alone (Cosman, 2014; Seeman, 2011), while the type of the antiresorptive or anabolic agent (Finkelstein et al., 2010; Cosman et al., 2011) as well as the optimal sequencing of the therapies remain discussed (Cosman et al., 2009; Muschitz et al., 2014; Whitmarsh et al., 2015; Cosman et al., 2017).

In the present study, we made use of quadruple labelled transiliac bone biopsy samples from postmenopausal osteoporotic patients for the characterization of bone matrix mineralization after either antiresorptive or anabolic therapy or a combination of both (Dempster et al., 2016b). These biopsy samples were obtained from women who had been previously treated with ALN and who received ongoing ALN plus concurrent treatment with teriparatide (TPTD) (alendronate treatment [ALN-Rx] arm), or from women whom TPTD was administered without prior or ongoing ALN (treatment-naïve [Rx-naïve] arm). These bone biopsy samples were previously characterized by histomorphometry (Dempster et al., 2016b) and the studied biopsy cohort represents a subgroup of a former study (Cosman et al., 2015) in which TPTD was given in two different regimens either cyclically or daily in the two aforementioned treatment arms. In the current work, the bone biopsy samples were measured for bone mineralization density distribution (BMDD) (Roschger et al., 2008), which is an important bone material quality influencing material stiffness (Currey, 1969) and which has been discussed in the context of bone fragility (Turner, 2002). Furthermore, the mineral content in areas between both younger and older double labels was analyzed for a characterization of the early secondary mineralization process.

2. Materials & methods

We analyzed 66 transiliac bone biopsy samples (ALN-Rx arm: $n = 37$, Rx-Naïve arm: $n = 29$) which were a subset of a previous study for bone histomorphometry (Dempster et al., 2016b). These were obtained from postmenopausal women (> 45 years old) with osteoporosis defined by a T score < -2.5 at spine, total hip or femoral neck, or a T score < -2 at any of these sites, with history of one or more osteoporosis-related fracture(s) or prevalent vertebral compression documented by spine radiographs (for clinical characteristics see Table 1).

Patients had to meet the following criteria to be included into the study. *ALN-Rx arm (patients with prior and ongoing ALN):* patients had to be on ALN at least for 1 year. *Rx-Naïve arm (patients without ALN):* Women enrolled in the Rx-Naïve cohort could not have been on any antiresorptive agent for at least 6 months before enrollment and could not have used a bisphosphonate for > 3 months within the prior 2 years and could not have used any IV bisphosphonate at any time.

Within each treatment arm (ALN-Rx arm or Rx-Naïve arm), volunteers were randomized to the biopsy before TPTD (these were the "no-TPTD" groups in the Tables 1 and 2) or to biopsy after daily TPTD or after cyclic TPTD. Thus, in the ALN-Rx arm, the patients remained on ALN alone or remained on ALN and were treated in combination with daily TPTD or with cyclic TPTD (cyclic treatment means 3 months on daily TPTD, 3 months off TPTD). A treatment protocol diagram is shown in the figure in Appendix A.

One transiliac bone biopsy sample was obtained from each patient in all treatment groups. The biopsy samples from the patients who received TPTD analyzed in this study were collected at 7 months after starting TPTD treatment. To prepare for biopsy, all patients were given quadruple labels: The first set of labels using tetracycline-HCl was administered at approximately 4.5 months into the study. Four weeks after completion of this first set of labels, a second set of labels was administered using demeclocycline-HCl. Both sets of labels were given in the same schedule: 3 days of tetracycline-HCl or demeclocycline-HCl, 12-day intermission, and then 3 more days of tetracycline-HCl or demeclocycline-HCl. Biopsy was performed 5 days after the last fluorochrome label was administered. Given this labelling sequencing, the tissue age of the bone matrix between the second (younger) set of labels is 8 to 20 days, the tissue age of the matrix between the first (older) set of labels is 54 to 66 days.

In the present work, we used previously assessed outcomes of bone histomorphometry for correlation with the bone mineralization data. All histomorphometric variables were defined and expressed according to the recommendations of the ASBMR nomenclature committee (Parfitt et al., 1987) and a more recent update (Dempster et al., 2013). Mineralizing surface (MS/BS) was calculated as double-label length plus half single-label length. If no labels were found, MS/BS were measured as zero (Dempster et al., 2016b).

2.1. Quantitative backscatter electron imaging (qBEI)

For the qBEI analysis in the scanning electron microscope, the polymethylmethacrylate embedded block samples from the previous histomorphometric study (Dempster et al., 2016b) were prepared to obtain planoparallel, polished, and carbon coated surfaces. In calibrated qBEI images of bone (as shown in Figs. 1 and 2) the backscattered electron intensities/pixel grey levels are proportional to the local percentage of calcium (Ca) in the bone material (for calibration procedure and other details of the method see a previous work (Roschger et al., 1998)). Briefly, for grey level calibration a carbon sample (reference for atomic number of 6) was set to grey level 25 and an aluminium sample (reference for atomic number 13) to grey level 225.

Table 1
Clinical and histomorphometric characteristics.

		ALN-Rx arm			Rx-Naïve arm		
		no TPTD $n = 14$	Cyclic TPTD n = 14	Daily TPTD $n = 9$	no TPTD n = 14	Cyclic TPTD $n = 7$	Daily TPTD $n = 8$
Baseline[a]	Age (years)[a]	64.0 (8.9)	68.8 (9.7)	67.0 (13.7)	61.0 (11.1)	61.4 (9.1)	65.8 (6.7)
	Years from menopause[a]	13.1 (10.0)	21.6 (13.1)	22.0 (15.7)	14.1 (12.1)	12.4 (12.0)	16.0 (8.3)
At biopsy	BMD spine (g/cm^2)	0.889 (0.057)	0.863 (0.122)	0.926 (0.085)	0.892 (0.097)	0.845 (0.084)	0.891 (0.098)
	BV/TV (%)	12.7 (4.7)	11.3 (3.7)	14.8 (5.3)	13.1 (4.6)	14.3 (5.6)	13.5 (3.7)
	MS/BS (%)	0.64 (0.58)	1.48 (0.98)	2.22 (2.15)	3.78 (2.43)	4.70 (3.46)	6.78 (5.54)

Data represent mean (SD) of the cohort measured for BMDD. Data of the entire study cohort were published previously (Dempster et al., 2016b; Cosman et al., 2015).
[a] At screening.

Table 2
BMDD outcomes from patients.

	ALN-Rx arm (with ALN)				Rx-Naïve arm (without ALN)				2 Way ANOVA		
	no TPTD (n = 14)	cyclic TPTD (n = 14)	daily TPTD (n = 9)	ALN-Rx pooled (n = 37)	no TPTD (n = 14)	cyclic TPTD (n = 7)	daily TPTD (n = 8)	Rx-Naïve pooled (n = 29)	interaction	factor A	factor B
Cn.CaMean (wt%Ca)	22.54 (0.69)	22.82 (0.43)	23.21 (0.23)	22.81 (0.57)	22.08 (0.44)	22.23 (0.47)	22.12 (0.94)	22.13 (0.60)	n.s.	< 0.001	n.s.
Cn.CaPeak (wt%Ca)	23.23 (0.62)	23.53 (0.45)	23.84 (0.28)	23.49 (0.53)	22.91 (0.44)	23.00 (0.46)	22.92 (1.01)	22.94 (0.63)	n.s.	< 0.001	n.s.
Cn.CaWidth (Δwt%Ca)	3.68 (0.59)	3.57 0.27	3.47 (0.31)	3.58 (0.43)	4.01 (0.40)	3.96 (0.53)	4.27 (0.42)	4.07 (0.44)	n.s.	< 0.001	n.s.
Cn.CaLow (%mdB.Ar)	4.65 (1.64)	4.33 (0.89)	3.68 (0.73)	4.29 (1.23)	5.52 (0.96)	5.31 (1.14)	5.66 (2.35)	5.50 (1.45)	n.s.	< 0.001	n.s.
Cn.CaHigh (%mdB.Ar)	10.70 (6.12)	13.32 (5.46)	16.86 (5.46)	13.19 (6.06)	7.46 (3.16)	8.12 (2.44)	9.67 (7.41)	8.23 (4.53)	n.s.	< 0.001	0.042*
Ct.CaMean (wt%Ca)	22.62 (0.58)	22.84 (0.50)	23.12 (0.25)	22.83 (0.51)	22.08 (0.61)	22.33 (0.68)	22.34 (0.77)	22.21 (0.66)	n.s.	< 0.001	n.s.
Ct.CaPeak (wt%Ca)	23.23 (0.60)	23.48 (0.44)	23.71 (0.29)	23.45 (0.50)	22.91 (0.56)	23.14 (0.67)	23.30 (0.67)	23.07 (0.62)	n.s.	0.014	0.043*
Ct.CaWidth (Δwt%Ca)	3.57 (0.29)	3.66 (0.32)	3.60 (0.34)	3.62 (0.31)	4.09 (0.67)	4.41 (0.69)	4.33 (0.37)	4.24 (0.61)	n.s.	< 0.001	n.s.
Ct.CaLow (%mdB.Ar)	3.61 (0.74)	3.52 (1.03)	3.06 (0.43)	3.43 (0.82)	5.35 (1.94)	5.46 (1.97)	5.83 (2.62)	5.50 (2.07)	n.s.	< 0.001	n.s.
Ct.CaHigh (%mdB.Ar)	9.90 (6.00)	12.15 (5.05)	14.96 (3.49)	12.04 (5.34)	6.90 (3.70)	10.35 (4.78)	11.43 (6.32)	8.97 (5.01)	n.s.	0.037	0.011*

Data are mean (SD). Factor A = ALN vs. without ALN, Factor B = no TPTD vs. cyclic TPTD vs. daily TPTD.
* Post hoc Tukey tests following Two-Way ANOVA revealed significant difference ($p < 0.05$) between daily TPTD versus no TPTD.

Fig. 1. qBEI images and BMDD. Entire cross-sectional area of the transiliac biopsy sample which was used for the assessment of BMDD from cancellous and cortical compartments separately (top). Examples of cancellous BMDD from 3 patients each of ALN-Rx and from Rx-Naïve arm (bottom).

2.1.1. Bone mineralization density distribution (BMDD)

The grey level histograms derived from qBEI images of bone tissue represent frequency distributions of pixels with a certain Ca content, in weight%, referred to as the bone mineralization density distribution (BMDD). The entire bone tissue area was recorded in a series of images about 2 mm × 2.5 mm covering the entire sectioned area of the bone biopsy sample (Fig. 1) using a Zeiss DSM 962 instrument (Zeiss, Oberkochen, Germany) equipped with a four-quadrant semiconductor backscatter electron detector. The instrument was operated at the following parameters: 20 kV accelerating voltage for the beam electrons, 110 pA probe current, 15 mm working distance, 50× nominal magnification corresponding to a pixel resolution of 3.6 μm and a scan speed of 100 s per frame. The BMDD was obtained from cancellous (Cn.) and cortical (Ct.) bone separately (Fig. 1) (Roschger et al., 2008; Roschger et al., 2003; Misof et al., 2014) and characterized by five parameters: The weighted mean Ca-concentration of the bone area (CaMean), the peak position of the histogram (CaPeak, indicating the most frequently measured Ca concentration), the full width at half maximum of the distribution (CaWidth, describing the heterogeneity in matrix mineralization), the percentage of bone areas having a Ca-concentration lower than 17.68 wt% Ca (CaLow), and the percentage of

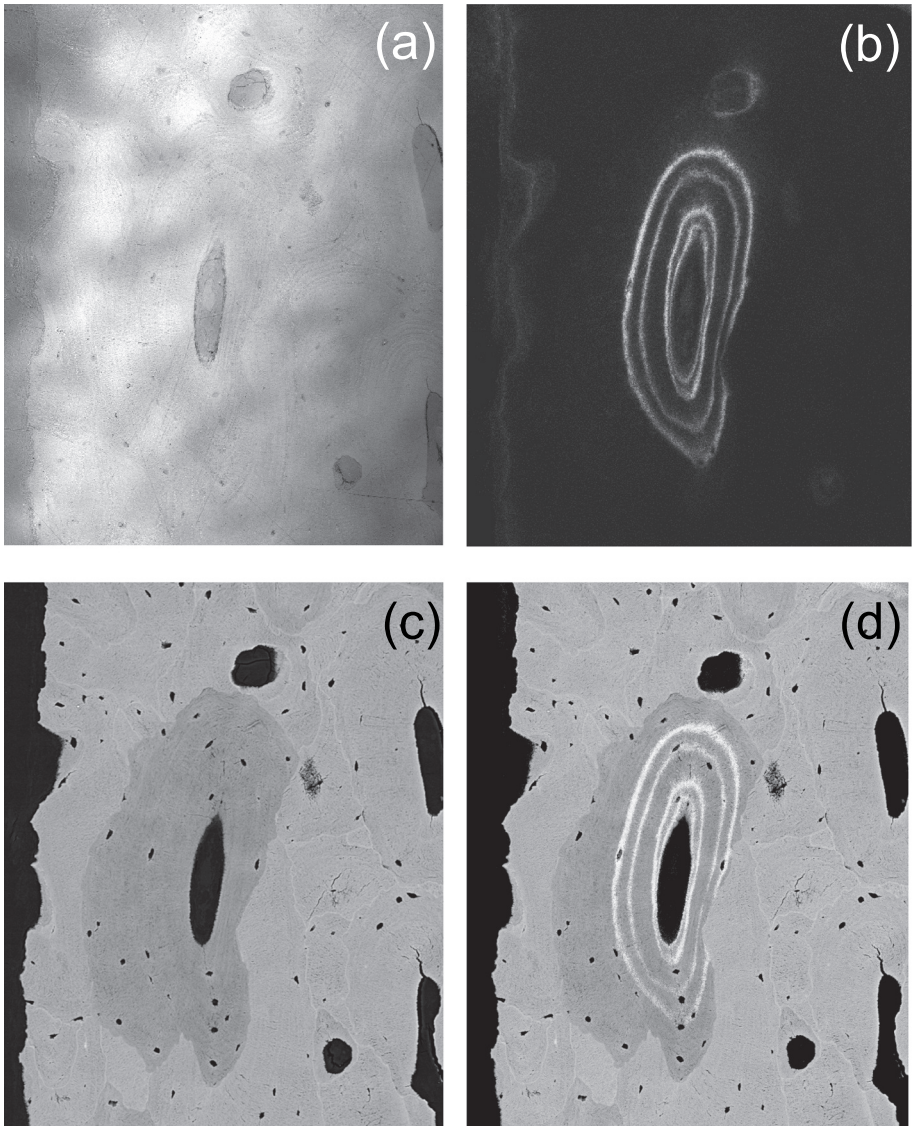

Fig. 2. Combination of CLSM and qBEI images. Measurement procedure shown in an example of an osteon: (a) CLSM image in reflection mode for the identification of the sample surface, (b) CLSM image of the two sets of double labels, (c) qBEI image, and (d) matched images.

bone areas having a Ca-concentration higher than 25.30 wt% Ca (Ca-High, corresponding to fully mineralized bone areas, mainly interstitial bone).

2.1.2. Mineral content at bone forming sites - Combination of qBEI with confocal scanning laser microscopy (CLSM)

For the visualisation of quadruple labels we imaged our block samples prior to carbon coating in a Confocal Laser Scanning Microscope (Leica TCS SP5, Leica Microsystems CMS GmbH, Wetzlar, Germany) using a laser light of 405 nm for fluorescence excitation and a 20× object lens (pixel resolution of 0.76 μm). For the exact matching of the qBEI with the CLSM images the focal plane of the CLSM had to be adjusted close to the bone sample surface. This was accomplished by identification of the sample surface with the reflected light signal (Fig. 2a) recorded in parallel with the fluorescence light (Fig. 2b). The bone areas with quadruple labels were then imaged using a Zeiss Supra 40 instrument (Zeiss, Oberkochen Germany) equipped with a four-quadrant semiconductor backscatter electron detector and operated at the following instrumental parameters: 20 kV accelerating voltage for the beam electrons, about 280 pA probe current, 10 mm working distance, 130× (or higher) nominal magnification corresponding to a pixel resolution of at least 0.88 μm, and a scan speed of 100 s per frame (Fig. 2c). By matching the CLSM images (Fig. 2b) with the qBEI images, the sites of the fluorescence labels were overlaid exactly onto the qBEI images (Fig. 2d).

This procedure allowed to record mineralization profiles following a straight line perpendicular to the mineralization front, from the young osteoid into mature bone (see line-profile in Fig. 3a and b). Further it enabled to measure the mean Ca content (in wt%) at sites of three different tissue ages: The bone area between the second set of labels (traced by yellow line, Fig. 3c) represented the mineral content of newly formed, young bone material (Ca_DL2) and between the first set of labels (traced by turquois line, Fig. 3c) represented the mineral content of older bone material (Ca_DL1). Additionally, the Ca content in highly mineralized, non-labelled bone packets (traced by pink line, Fig. 3c) was analyzed representing interstitial bone (Ca_int) with the highest mineral content (plateau level) in the bone sample. The analyzed median (25th; 75th percentiles) area between double labels was 2284.5 (1319.9; 4450.8) μm^2. Altogether 335 areas between double labels were analyzed (about 16 areas per each sample), thus a total area of 0.77 mm^2 was analyzed for Ca_DL2 or Ca_DL1. For information about the mineral content of interstitial bone, the median (25th; 75th

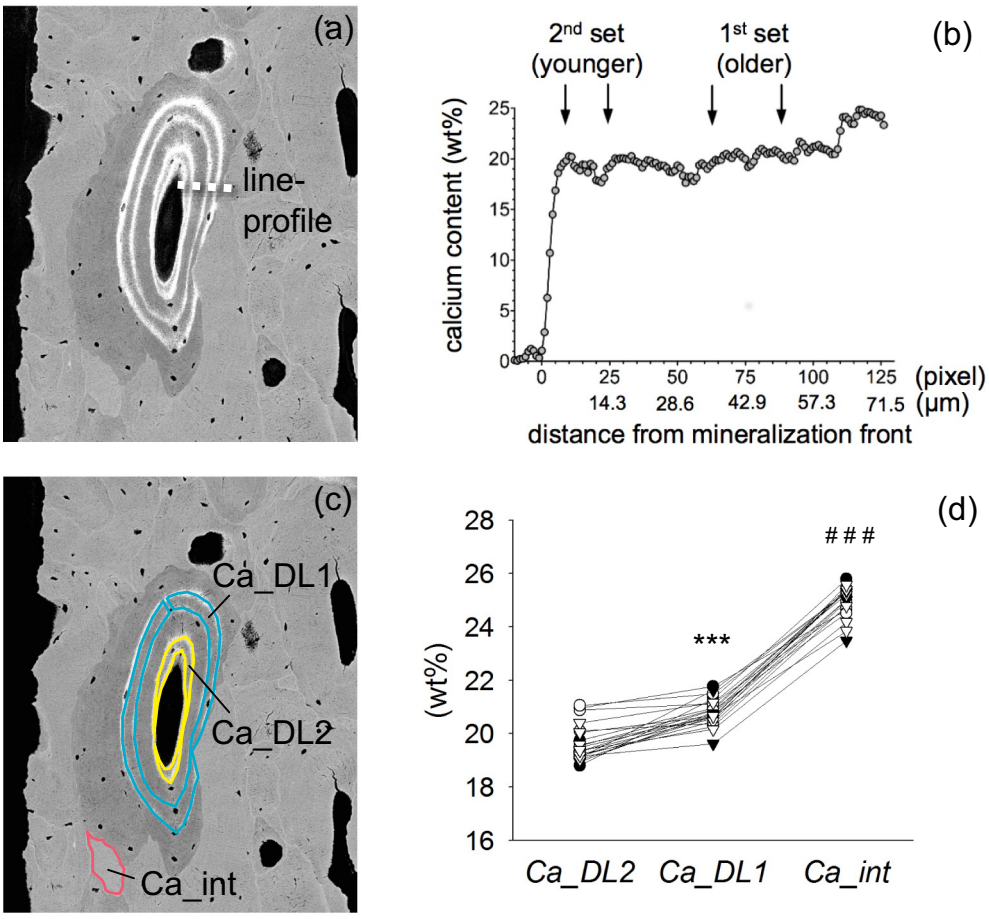

Fig. 3. Information deduced from the matched images: (a) Region of the mineralization profile (shown in (b)) indicated by the dotted line. (b) Line profile demonstrating the increase in mineral content with increasing distance from the mineralization front (arrows show the site of the labels). (c) traced areas for Ca_DL2 (younger set of double labels, shown in yellow), Ca_DL1 (older set of double labels, shown in turquois), and traced area for Ca_int (indicative for older, highly mineralized interstitial bone, indicated in pink). (d) Analysis of mineralization kinetics: Mean Ca_DL2, Ca_DL1, and Ca_int for each sample. Circles indicate ALN-Rx arm, triangles Rx-Naïve arm, black indicates ALN-Rx Control or Rx-Naïve Control, white indicates cyclic TPTD or daily TPTD. $^{***}p < 0.001$ versus Ca_DL2, $^{###}p < 0.001$ versus Ca_DL1.

percentiles) area was 2553.4 (1116.8; 5761.5) µm^2. Overall 129 areas of interstitial bone were measured (about 6 areas per each sample) which represents in total an area of 0.33 mm^2 for information about Ca_int.

This analysis at specific bone sites of known mineralized tissue age was done in samples chosen by highest MS/BS of the respective group (ensuring sufficient numbers of quadruple labels for analysis) from the Rx-ALN arm: $n = 4$ ALN-Rx Control, n = 4 ALN-Rx cyclic TPTD, $n = 2$ ALN-Rx daily TPTD; and Rx-Naïve arm: n = 4 Rx-Naïve Control, n = 4 Rx-Naïve cyclic TPTD, and $n = 3$ Rx-Naïve daily TPTD. All image evaluations were performed using ImageJ software (version 1.50f; NIH, Bethesda, MD, USA) (Schneider et al., 2012) by applying custom made routines.

2.2. Statistical analysis

Statistical analysis was performed using SigmaStat for Windows Version 4.0 (SPSS Inc.). Comparison of the BMDD parameters was performed using two-way ANOVA comparison with factor A = ALN treatment (ALN vs. No-ALN, i.e. ALN-Rx treatment arm pooled versus Rx-Naïve treatment arm pooled) and factor B = No-TPTD/cyclic-TPTD/daily-TPTD (i.e. comparison of ALN and Rx-Naïve pooled with ALN-Rx cyclic TPTD and Rx-Naïve cyclic TPTD pooled with ALN-Rx daily TPTD and Rx-Naïve daily TPTD pooled) and subsequent Tukey post hoc tests. For characterization of mineralization kinetics, Ca_DL2, Ca_DL1, and Ca_int were averaged for each patient. Comparison of Ca_DL2, Ca_DL1, and Ca_int among the treatment groups is based on two-way ANOVA with factor A = ALN treatment and factor B = TPTD treatment (No-TPTD vs. TPTD, i.e. comparison between ALN and Rx-Naïve pooled with ALN-Rx cyclic TPTD, ALN-Rx daily TPTD, Rx-Naïve cyclic TPTD, and Rx-Naïve daily TPTD pooled). Two-way ANOVA used Shapiro-Wilk and Brown-Forsythe test for assumptions concerning normality and equal variance, respectively. Pairwise comparison of Ca_DL2 and Ca_DL1 is based on paired *t*-test. Correlation analyses are based on Pearson product moment (PPM) correlation. Two-sided $p < 0.05$ was considered significant.

3. Results

3.1. BMDD of total cancellous or cortical compartment: comparison by treatment

Two-Way ANOVA comparison for Cn. BMDD or Ct. BMDD is summarized in Table 2. No significant interaction between the two studied factors could be observed (factor A = ALN treatment and factor B = No-TPTD/cyclicTPTD/dailyTPTD) for any BMDD parameter. Comparison for Factor A showed significant differences for all BMDD-parameters. CaMean (+3.1% and +2.8%, in Cn. and Ct. bone, respectively, both $p < 0.001$), CaPeak (+2.4%, $p < 0.001$ and +1.6%, $p < 0.05$) and CaHigh (+60%, $p < 0.001$ and +34%, $p < 0.05$) were increased and CaWidth (−12% and −15%, both $p < 0.001$) and CaLow (−22% and −38%, both $p < 0.001$) were decreased in the ALN-Rx treatment arm compared to the naïve-Rx arm (see Table 2). Factor B showed weak significant differences for CaHigh (in both cancellous and cortical bone) and for CaPeak in cortical bone. Tukey post hoc comparison revealed that the latter were higher in daily TPTD compared to those without TPTD. Typical effects of TPTD treatment like an increase in CaWidth and CaLow were not observed, despite the increase in bone formation (i.e. increase in MS/BS) by TPTD (Table 1).

3.2. Mineral content at bone forming sites – characterization of early secondary mineralization

The mineralization profile from the young osteoid into mature bone (line-profile in Fig. 3a and b) shows that with increasing distance from the mineralization front (i.e. with increasing age of the matrix) the first increase in Ca concentration is steep (corresponding to the primary mineralization phase) which is followed by a flatter increase (corresponding to the secondary mineralization phase). By using the time information based on the position of the labels with respect to the line profile (Fig. 3b) it can be seen that bone between both sets of labels is already in the state of secondary mineralization, thus the primary mineralization process is already complete after 5 days once the mineralization has started (which is the time period from the last label to the biopsy procedure).

For quantitative characterization of the time course of Ca accumulation in the bone matrix, we assessed the mean Ca content at sites of defined tissue age between the younger or older double labels, respectively (Ca_DL2 and Ca_DL1). The mineralization kinetics are reflected by the increase in mineral content from the younger (corresponding to 8–20 days old matrix) Ca_DL2 to the older set of double labels (corresponding to bone matrix aged 54–66 days) Ca_DL1 and further to Ca_int in interstitial bone (Fig. 3c and d). Two-way ANOVA revealed that neither Ca_DL2 nor Ca_DL1 or Ca_int were influenced by ALN and/or TPTD. Thus, data from all treatment groups were pooled for general information on early secondary mineralization in postmenopausal osteoporosis. The mean mineral content in Ca_DL2 was 19.64 ± 0.68 wt% Ca (mean ± SD), Ca_DL1 was 20.80 ± 0.51 wt% Ca (corresponding to an average increase of +5.9% or 1.16 ± 0.63 wt % Ca within 46 days [mid of first double label until mid of second double label] during the early secondary mineralization). Ca_int was 24.98 ± 0.59 wt% Ca corresponding to an increase of +20.1% compared to Ca_DL1. Pairwise comparison of Ca_DL2 with Ca_DL1 revealed a significant difference: Ca_DL1 was higher than Ca_DL2 ($p < 0.001$), whereas Ca_int was higher than Ca_DL1 ($p < 0.001$).

Significant correlations between Ca_DL1 and Ca_DL2 (PPM $R = 0.46$, $p < 0.05$) (Fig. 4a), between Ca_DL1 and Ca_int (PPM $R = 0.46$, $p < 0.05$) (Fig. 4b), and between the difference of Ca_DL1 and Ca_DL2 with Ca_int (PPM $R = 0.53$, $p < 0.05$) were found while no significant correlation could be observed between Ca_int and Ca_DL2 (PPM $p > 0.05$). Furthermore, no significant correlation between Ca_DL2 or Ca_DL1 or the difference of both with histomorphometric indices of bone formation (mineralizing surface per bone surface, mineral apposition rate, bone formation rate per bone surface) could be observed (all PPM $p > 0.05$) (Fig. 4c and d).

4. Discussion

In this work, we present the first data on bone matrix mineralization from patients after combination of ongoing antiresorptive with concurrent anabolic therapy. This biopsy cohort was previously studied by histomorphometry, which gave evidence for the stimulation of bone turnover/formation by both cyclic and daily TPTD in patients with ongoing ALN treatment, as well as in patients on mono-therapy with cyclic or daily TPTD (Dempster et al., 2016b). The general differences found now in BMDD between the ALN-Rx and Rx-naïve treatment arm were in line with the typical changes in antiresorptive treatment (increase in CaMean, CaPeak and CaHigh, decrease in CaWidth and CaLow) reported in numerous previous studies (Roschger et al., 2014; Boivin and Meunier, 2002). In contrast none of the expected typical BMDD changes occurring during anabolic treatment with TPTD or PTH (decrease in CaMean, increase in CaWidth or at least an increase in CaLow due to enhanced bone formation) (Dempster et al., 2016a; Misof et al., 2003; Paschalis et al., 2005; Misof et al., 2010; Misof et al., 2016) could be observed in our cohort.

Additionally to the BMDD, we took advantage of the quadruple labelling of these biopsy samples for the characterization of the mineralization kinetics. The latter represents the time course of mineral accumulation within the newly formed matrix up to the plateau level of mineralization and is additionally to turnover a determinant of the BMDD (Roschger et al., 2008). In the present work, we analyzed the mineral content in the bone matrix of individual forming bone packets (bone structural units) at different well-defined mineralized tissue ages. Further, we also measured highly mineralized (oldest) interstitial bone (Ca_int) for information on the plateau-level of mineralization. In line with our previous observation (Roschger et al., 2008), we found that the rapid phase of primary mineralization was completed just before the occurrence of the second set of double labels. Thus Ca_DL2

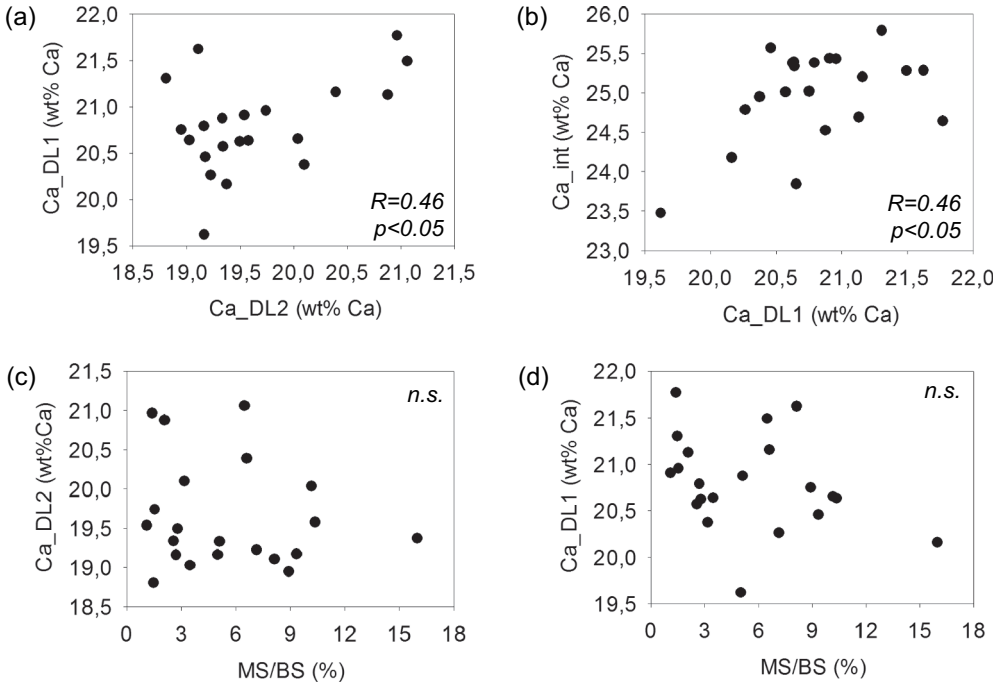

Fig. 4. Correlation between Ca_DL2, Ca_DL1_Ca_int and mineralizing surface per bone surface (MS/BS). (a) The mineral content between the first set of labels (Ca_DL1) plotted versus the mineral content between the second set of labels Ca_DL2. (b) The mineral content of interstitial bone Ca_int plotted versus Ca_DL1. (c) Ca_DL2 and (d) Ca_DL1 plotted versus MS/BS.

represented the Ca-content at the onset of the secondary mineralization phase at mineralized tissue age interval of 8 to 20 days, while Ca_DL1 represented the progress in mineral accumulation during the early secondary mineralization phase at a mineralized tissue age interval of 54 to 66 days.

The comparison of the time course of matrix mineralization between both treatment arms revealed no significant differences. This suggests that neither ALN nor TPTD interfered with the mineralization process. These data are limited by the small sample size studied. However, they are, consistent with the previous work by Fuchs and colleagues who studied the rate of secondary mineralization in rabbits and reported that bisphosphonates do not alter the secondary mineralization process (Fuchs et al., 2011). Less is known about potential effects of TPTD on the mineralization kinetics. A Raman microspectroscopy study reported TPTD effects on bone material properties in patients who were pre-treated with different types of bisphosphonates. However, neither time course of mineralization nor combination treatment were addressed in the latter work (Gamsjaeger et al., 2011).

As the measured secondary mineralization parameters Ca_DL2, Ca_DL1 and Ca_int were not influenced by ALN and/or TPTD we pooled the data from all for general information about early secondary mineralization parameters in postmenopausal osteoporosis. This might be useful for comparison in future analyses of secondary mineralization in standard labelled bone biopsy samples (having one set of double labels). Due to the quadruple labelling we could also calculate the early secondary mineralization rate being 0.18 wt% Ca per week. Assuming that this mineralization rate remains constant, the plateau value of mineral content (Ca_int) would be reached already within 23 weeks (~6 months). However, more likely the mineralization rate is gradually decreases with time to zero, when the plateau level of Ca_int is reached. Thus a much older tissue age in Ca_int has to be expected. This slowing down of secondary mineralization rate has been explicitly demonstrated in animal models where the plateau mineralization was achieved in ~55 weeks in rabbits (Fuchs et al., 2008) and ~90 weeks in ewes (Bala et al., 2010).

Our correlation analyses of individual Ca_DL2 with Ca_DL1 values showed that a lower initial mineralization level seems to be compensated by a somewhat higher initial mineralization rate. Noteworthy, neither the mineral content at the two studied tissue ages nor the rate of early secondary mineralization was correlated with bone turnover indices by histomorphometry. This suggests that the fundamental processes of bone matrix mineralization are independent of the number of bone multicellular units, which are active in an individual.

As our analysis of the mineralization kinetics did not give evidence for differences between those treated with TPTD compared to those without TPTD, our results cannot contribute to the explanation why we could not observe the typical BMDD effect in the TPTD treated. A reason for the latter lack of typical TPTD effects in the BMDD might be that the rather short duration of TPTD administration of 7 months which is comparable to the duration of about one bone remodelling cycle only (Kenkre and Bassett, 2018). It should be noted that the even higher typical degree of mineralization and increased portion of highly mineralized bone area after daily TPTD treatment is an aberrant finding which is in contrast to all of our previous studies reporting effects of anabolic treatment on bone mineralization (Dempster et al., 2016a; Misof et al., 2003; Misof et al., 2010; Misof et al., 2016). As the peak calcium concentration represents mainly the bulk bone material, it is unlikely that this is an effect of 7 months treatment. It seems more likely that the patients of this study group had already highly increased bone matrix mineralization before administration of TPTD. However, the reason for these potentially increased baseline levels remain unknown.

Our study has some limitations. The design did not provide a group with concurrently started ALN and TPTD. Thus, in the ALN-Rx arm TPTD was given to patients who had already decreased bone turnover by the previous ALN treatment. Therefore concurrent start with ALN and TPTD might have a different effect on BMDD. However, as ALN is the first line therapy in postmenopausal osteoporosis, treatment with TPTD in patients already treated with ALN comparable to our study design might be the more typical situation. Furthermore, the total number of analyzed biopsy samples was rather high, the sample size within each of the study groups was modest. In particular, for the analysis of the calcium content between the double labels, the presence of the latter was the prerequisite, which was not the case in a relatively high number of ALN treated samples. Thus for this analysis only about a third of the total number of samples was studied which limits the power of detecting differences. On the other hand, the availability of two double labels in human bone samples is rare and therefore the reported information on the time course of mineralization is unique. Furthermore, considering the short time period of treatment, a paired biopsy design might have been more successful to demonstrate eventual changes in BMDD due to TPTD treatment. Paired biopsy samples might have been also an advantage for finding differences in the mineralization kinetics due to treatment.

In conclusion, we could for the first time follow the time course of mineral content with tissue age in human bone after ALN, TPTD or concurrent treatment with both using the information from the two sets of double fluorescence labels. We found no evidence that any of the studied types of treatment altered the time course of secondary mineralization in bone. Considering the BMDD outcomes, we could observe a generally higher degree of mineralization in the patients who received prior and ongoing ALN reflecting the lower bone turnover in these individuals compared to those without ALN treatment. However, 7 months of cyclic or daily TPTD treatment seemed to be too short to cause the expected typical effects on the BMDD in a non-paired biopsy study cohort.

Supplementary data to this article can be found online at https://doi.org/10.1016/j.bonr.2020.100253.

Transparency document

The Transparency document associated with this article can be found, in online version.

Acknowledgments

The authors thank D. Gabriel, P. Keplinger, S. Lueger, and P. Messmer for technical assistance with sample preparation, CLSM and qBEI measurements at the Bone Material Laboratory of the Ludwig Boltzmann Institute of Osteology, Vienna, Austria. This work was supported by the AUVA (Austrian Social Insurance for Occupational Risk) and the ÖGK (Austrian Social Health Insurance Fund). The TPTD used in this study was graciously provided by Eli Lilly & Co. The study was supported by NIH grant R01 AR056651.

Authors' roles

Study design: FC, JWN, RL, KK, DWD. Study conduct: FC, RL, MB. Data collection: BMM, PR, HZ. Data analysis: BMM, PR. Data interpretation: BMM, PR, DWD. Drafting manuscript: BMM, PR, DWD. Revising manuscript content: BMM, PR, KK, DWD. Approving final version of the manuscript: BMM, PR, HZ, JWN, MB, FC, RL, KK, DWD. BMM and PR take responsibility for the integrity of the data analysis.

Declaration of competing interest

JN has received medication for research studies from Eli Lilly and Co and Radius Health. FC is an advisor, consultant and speaker for Radius Health and Amgen. She was an advisor, consultant, and speaker for Eli Lilly (no longer active) and an advisor for Merck (no longer active). RL has served as a consultant for Eli Lilly & Co. DWD has received research funds from Eli Lilly & Company, Amgen Inc., and

Radius Health. He has served as a consultant for Merck & Co., Amgen Inc., NPS Pharmaceuticals, Radius Health, Tarsa Pharmaceuticals, and Eli Lilly & Co., and on speakers bureaus for Eli Lilly & Co., Amgen Inc., and Radius Health. BMM, PR, HZ, MB and KK state that they have no conflicts of interest.

References

Bala, Y., Farlay, D., Delmas, P.D., Meunier, P.J., Boivin, G., 2010. Time sequence of secondary mineralization and microhardness in cortical and cancellous bone from ewes. Bone 46, 1204–1212.

Boivin, G., Meunier, P.J., 2002. Effects of bisphosphonates on matrix mineralization. J. Musculoskelet. Neuronal Interact. 2, 538–543.

Cosman, F., 2014. Anabolic and antiresorptive therapy for osteoporosis: combination and sequential approaches. Curr Osteoporos Rep 12, 385–395. https://doi.org/10.1007/s11914-014-0237-9.

Cosman, F., Wermers, R.A., Recknor, C., Mauck, K.F., Xie, L., Glass, E.V., Krege, J.H., 2009. Effects of teriparatide in postmenopausal women with osteoporosis on prior alendronate or raloxifene: differences between stopping and continuing the anti-resorptive agent. J. Clin. Endocrinol. Metab. 94, 2780–3772.

Cosman, F., Eriksen, E.F., Recknor, C., Miller, P.D., Guañabens, N., Kasperk, C., Papanastasiou, P., Readie, A., Rao, H., Gasser, J.A., Bucci-Rechtweg, C., Boonen, S., 2011. Effects of intravenous zoledronic acid plus subcutaneous teriparatide [rhPTH (1-34)] in postmenopausal osteoporosis. J. Bone Miner. Res. 26, 503–511. https://doi.org/10.1002/jbmr.238.

Cosman, F., Nieves, J.W., Zion, M., Garrett, P., Neubort, S., Dempster, D., Lindsay, R., 2015. Daily or cyclical teriparatide treatment in women with osteoporosis on no prior therapy and women on alendronate. J. Clin. Endocrinol. Metab. 100, 2769–2776. https://doi.org/10.1210/jc.2015-1715.

Cosman, F., Nieves, J.W., Dempster, D., 2017. Treatment sequence matters: anabolic and antiresorptive therapy for osteoporosis. J. Bone Miner. Res. 32, 198–202. https://doi.org/10.1002/jbmr.3051.

Currey, J.D., 1969. The mechanical consequences of variation in the mineral content of bone. J. Biomech. 2, 1–11.

Dempster, D.W., Compston, J.E., Drezner, M.K., Glorieux, F.H., Kanis, J.A., Malluche, H., Meunier, P.J., Ott, S.M., Recker, R.R., Parfitt, A.M., 2013. Standardized nomenclature, symbols, and units for bone histomorphometry: a 2012 update of the report of the ASBMR Histomorphometry Nomenclature Committee. J. Bone Miner. Res. 28, 2–17.

Dempster, D.W., Roschger, P., Misof, B.M., Zhou, H., Paschalis, E.P., Alam, J., Ruff, V.A., Klaushofer, K., Taylor, K.A., 2016a. Differential effects of teriparatide and zoledronic acid on bone mineralization density distribution at 6 and 24 months in the SHOTZ study. J. Bone Miner. Res. 31, 1527–1535. https://doi.org/10.1002/jbmr.2825.

Dempster, D.W., Cosman, F., Zhou, H., Nieves, J.W., Bostrom, M., Lindsay, R., 2016b. Effects of daily or cyclic teriparatide on bone formation in the iliac crest in women on no prior therapy and in women on alendronate. J. Bone Miner. Res. 31, 1518–1526. https://doi.org/10.1002/jbmr.2822.

Finkelstein, J.S., Wyland, J.J., Lee, H., Neer, R.M., 2010. Effects of teriparatide, alendronate, or both in women with postmenopausal osteoporosis. J. Clin. Endocrinol. Metab. 95, 1838–1845. https://doi.org/10.1210/jc.2009-1703.

Fuchs, R.K., Allen, M.R., Ruppel, M.E., Diab, T., Phipps, R.J., Miller, L.M., Burr, D.B., 2008. In situ examination of the time-course for secondary mineralization of Haversian bone using synchrotron Fourier transform infrared microspectroscopy. Matrix Biol. 27, 34–41.

Fuchs, R.K., Faillace, M.E., Allen, M.R., Phipps, R.J., Miller, L.M., Burr, D.B., 2011. Bisphosphonates do not alter the rate of secondary mineralization. Bone 49, 701–705.

Gamsjaeger, S., Buchinger, B., Zoehrer, R., Phipps, R., Klaushofer, K., Paschalis, E.P., 2011. Effects of one year daily teriparatide treatment on trabecular bone material properties in postmenopausal osteoporotic women previously treated with alendronate or risedronate. Bone 49, 1160–1165. https://doi.org/10.1016/j.bone.2011.08.015.

Kenkre, J.S., Bassett, J., 2018. The bone remodelling cycle. Ann. Clin. Biochem. 55, 308–327. https://doi.org/10.1177/0004563218759371.

Misof, B.M., Roschger, P., Cosman, R., Kurland, E.S., Tesch, W., Messmer, P., Dempster, D.W., Nieves, J., Shane, E., Fratzl, P., Klaushofer, K., Bilezikian, J., Lindsay, R., 2003. Effects of intermittent parathyroid hormone administration on bone mineralization density distribution in iliac crest biopsies from patients with osteoporosis: a paired study before and after treatment. J. Clin. Endocrinol. Metab. 88, 1150–1156.

Misof, B.M., Paschalis, E.P., Blouin, S., Fratzl-Zelman, N., Klaushofer, K., Roschger, P., 2010. Effects of 1 year of daily teriparatide treatment on iliacal bone mineralization density distribution (BMDD) in postmenopausal osteoporotic women previously treated with alendronate or risedronate. J. Bone Miner. Res. 25, 2297–2303. https://doi.org/10.1002/jbmr.198.

Misof, B.M., Dempster, D.W., Zhou, H., Roschger, P., Fratzl-Zelman, N., Fratzl, P., Silverberg, S.J., Shane, E., Cohen, A., Stein, E., Nickolas, T.L., Recker, R.R., Lappe, J., Bilezikian, J.P., Klaushofer, K., 2014. Relationship of bone mineralization density distribution (BMDD) in cortical and cancellous bone within the iliac crest of healthy premenopausal women. Calcif. Tissue Int. 95, 332–339.

Misof, B.M., Roschger, P., Dempster, D.W., Zhou, H., Bilezikian, J.P., Klaushofer, K., Rubin, M.R., 2016. PTH(1-84) administration in hypoparathyroidism transiently reduces bone matrix mineralization. J. Bone Miner. Res. 31, 180–189. https://doi.org/10.1002/jbmr.2588.

Muschitz, C., Kocijan, R., Fahrleitner-Pammer, A., Pavo, I., Haschka, J., Schima, W., Kapiotis, S., Resch, H., 2014. Overlapping and continued alendronate or raloxifene administration in patients on teriparatide: effects on areal and volumetric bone mineral density—the CONFORS study. J. Bone Miner. Res. 29, 1777–1785. https://doi.org/10.1002/jbmr.2216.

Parfitt, A.M., Drezner, M.K., Glorieux, F.H., Kanis, J.A., Malluche, H., Meunier, P.J., Ott, S.M., Recker, R.R., 1987. Bone histomorphometry: standardization of nomenclature, symbols, and units. Report of the ASBMR Histomorphometry Nomenclature Committee. J. Bone Miner. Res. 2, 595–610.

Paschalis, E.P., Glass, E.V., Donley, D.W., Eriksen, E.F., 2005. Bone mineral and collagen quality in iliac crest biopsies of patients given teriparatide: new results from the fracture prevention trial. J. Clin. Endocrinol. Metab. 90, 4644–4649.

Roschger, P., Fratzl, P., Eschberger, J., Klaushofer, K., 1998. Validation of quantitative backscattered electron imaging for the measurement of mineral density distribution in human bone biopsies. Bone 23, 319–326.

Roschger, P., Gupta, H.S., Berzlanovich, A., Ittner, G., Dempster, D.W., Fratzl, P., Cosman, F., Parisien, M., Lindsay, R., Nieves, J.W., Klaushofer, K., 2003. Constant mineralization density distribution in cancellous human bone. Bone 32, 316–323.

Roschger, P., Paschalis, E.P., Fratzl, P., Klaushofer, K., 2008. Bone mineralization density distribution in health and disease. Bone 42, 456–466.

Roschger, P., Misof, B., Paschalis, E., Fratzl, P., Klaushofer, K., 2014. Changes in the degree of mineralization with osteoporosis and its treatment. Curr Osteoporos Rep 12, 338–350 (Review).

Schneider, C.A., Rasband, W.S., Eliceiri, K.W., 2012. NIH image to ImageJ: 25 years of image analysis. Nat. Methods 9, 671–675.

Seeman, E., 2011. PERSPECTIVES Anabolic Plus Antiresorptive: Is One Plus One More or Less Two? IBMS BoneKEy 8, 221–228. http://www.bonekey-ibms.org/cgi/content/full/ibmske;8/5/221 https://doi.org/10.1138/20110510.

Turner, C.H., 2002. Biomechanics of bone: determinants of skeletal fragility and bone quality. Osteoporos. Int. 13, 97–104.

Whitmarsh, T., Treece, G.M., Gee, A.H., Poole, K.E., 2015. Mapping bone changes at the proximal femoral cortex of postmenopausal women in response to alendronate and teriparatide alone, combined or sequentially. J. Bone Miner. Res. 30, 1309–1318. https://doi.org/10.1002/jbmr.2454.